Dispersion of repolarization in cardiac resynchronization therapy

Bart Hooft van Huysduynen, MD, Cees A. Swenne, PhD, Jeroen J. Bax, MD, Gabe B. Bleeker, MD, Harmen H.M. Draisma, MSc, Lieselot van Erven, MD, Sander G. Molhoek, MD, Hedde van de Vooren, MSc, Ernst E. van der Wall, MD, Martin J. Schalij, MD

From the Department of Cardiology, Leiden University Medical Center, Leiden, The Netherlands.

BACKGROUND Proarrhythmic effects of cardiac resynchronization therapy (CRT) as a result of increased transmural dispersion of repolarization (TDR) induced by left ventricular (LV) epicardial pacing in a subset of vulnerable patients have been reported. The possibility of identifying these patients by ECG repolarization indices has been suggested.

OBJECTIVES The purpose of this study was to test whether repolarization indices on the ECG can be used to measure dispersion of repolarization during pacing.

METHODS CRT devices of 28 heart failure patients were switched among biventricular, LV, and right ventricular (RV) pacing. ECG indices proposed to measure dispersion of repolarization were calculated. The effects of CRT on repolarization were simulated in ECGSIM, a mathematical model of electrocardiogram genesis. TDR was calculated as the difference in repolarization time between the epicardial and endocardial nodes of the heart model.

RESULTS *Patients:* The interval from the apex to the end of the T wave was shorter during biventricular pacing (102 $\pm$ 18 ms) and LV pacing (106 $\pm$ 21 ms) than during RV pacing (117 $\pm$ 22 ms, $P \leq .005$). T-wave amplitude and area were low during biventricular pacing (287 $\pm$ 125 μV and 56 $\pm$ 22 μV $\cdot$ s, respectively, $P = .0006$ vs RV pacing). T-wave complexity was high during biventricular pacing (0.42 $\pm$ 0.26, $P = .004$ vs RV pacing). *Simulations:* Repolarization patterns were highly similar to the preceding depolarization patterns. The repolarization patterns of different pacing modes explained the observed magnitudes of the ECG repolarization indices. Average and local TDR were not different between pacing modes.

CONCLUSION In patients treated with CRT, ECG repolarization indices are related to pacing-induced activation sequences rather than transmural dispersion. TDR during biventricular and LV pacing is not larger than TDR during conventional RV endocardial pacing.

KEYWORDS Dispersion of repolarization; Resynchronization therapy; Arrhythmogenesis; Electrocardiography; Computer modeling

(Heart Rhythm 2005;2:1286–1293)

Introduction

Cardiac resynchronization therapy (CRT) restores coordinated mechanical contraction in most heart failure patients with compromised intraventricular conduction.[1,2] Application of CRT reduces the occurrence of heart failure[3] and all-cause mortality.[4] However, CRT may have proarrhythmic effects as a result of increased dispersion of repolarization in a subset of vulnerable patients.[5,6] Left ventricular (LV) epicardial pacing reverses the natural activation from endocardium to epicardium. This advances the repolarization time of the already short epicardial action potentials, thereby increasing repolarization time differences with the longer underlying action potentials of the midmyocardial and endocardial layers. Thus, increased transmural dispersion of repolarization (TDR) may enhance susceptibility to arrhythmias. The ability to identify vulnerable patients using a noninvasive repolarization measure on the ECG, such

Supported by Grant 2001.177 from the Netherlands Heart Foundation, The Hague.

Address reprint requests and correspondence: Dr. Cees A. Swenne, Department of Cardiology, Leiden University Medical Center, PO Box 9600, 2300 RC Leiden, The Netherlands.

E-mail address: c.a.swenne@lumc.nl.

(Received May 12, 2005; accepted August 25, 2005.)

1547-5271/$ -see front matter doi:10.1016/j.hrthm.2005.08.031

Table 1 Patient characteristics

Gender (male/female)	22/6
Age (yr)	68.5 ± 8.1
Etiology (ischemic/nonischemic)	17/11
New York Heart Association functional class	3.0 ± 0.5
Minnesota Quality of Life Score	43 ± 13
Six-minute walking distance (m)	254 ± 119
Ejection fraction (%)	21 ± 7

as the interval from T-wave apex to T-wave end (Tapex–end), would be of great clinical value.[7]

The Tapex–end interval as a measure of dispersion of repolarization was proposed based on experiments in a wedge preparation of the LV wall.[8] Although the wedge preparation is a valuable research tool, it represents only part of the heart, and the pseudo-ECG derived from the preparation probably is not representative of clinical ECGs. Other proposed ECG indices of dispersion of repolarization are difficult to verify *in vivo,* because in most studies either epicardial or endocardial repolarization is recorded from a limited number of electrodes on the heart.[9,10]

In the current study, we used ECGSIM,[11] a whole-heart model of ECG simulation, to study whether epicardial pacing in CRT increases TDR. Moreover, we sought to clarify how the repolarization process during CRT is reflected in ECG indices proposed to measure dispersion of repolarization.

Methods

Patients

Twenty-eight heart failure patients were studied 2 days after they underwent implantation of a biventricular pacemaker at the Leiden University Medical Center. Patient characteristics are listed in Table 1. After the patients had rested supine for 5 minutes, standard 12-lead ECGs were recorded continuously while the pacemaker was programmed in random order to biventricular pacing, LV pacing, right ventricular (RV) pacing and no pacing mode. All modes were kept for 3 minutes. The last minute of the ECG recordings in any mode was analyzed.

ECG analysis was performed by LEADS (Leiden ECG Analysis and Decomposition Software), our MATLAB (The MathWorks, Natick, MA, USA) program for research-oriented ECG analysis. LEADS first computed an averaged beat in order to minimize noise. In this averaged beat, the beginning and end of the QRS complex were automatically detected. An observer, who was blinded to the patient data, corrected this interval if necessary. LEADS identified the apex and end of the T wave in each ECG lead. The end of the T wave was set at the point where the tangent to the steepest portion of the terminal part of the T wave crossed the isoelectric line. Subsequently, LEADS searched backward for the apex of the T wave, defined as the point of the T wave with the highest amplitude. Finally, LEADS calculated a number of ECG indices proposed to assess dispersion of repolarization: Tapex–end interval,[8] QT interval,[12] T-wave amplitude,[13] T-wave surface area,[14] and T-wave complexity.[15] QT and Tapex–end intervals were corrected for heart rate using the Bazett formula.[16] T-wave complexity was calculated by singular value decomposition of the T wave.[15,17] The higher, more complex, singular values 2 to 8 were divided by the first, most simple component to quantify T-wave complexity. In addition, LEADS constructed the vectorcardiogram by using the inverse Dower matrix[18,19] and calculated the spatial angle between the QRS and T axes.

Simulations

ECGSIM is an ECG simulation program that consists of a mathematical whole heart model placed in a human thorax.[11] The model geometry is based on magnetic resonance images of heart and thorax, containing conduction inhomogeneities such as the lungs. Surfaces of the LV and RV consist of 257 epicardial and endocardial nodes. A transmembrane action potential in each node represents local electrical activity.[13] The naturally present TDR is incorporated in the model. The epicardium has shorter action potential durations than the endocardium, so the epicardium repolarizes earlier despite earlier endocardial activation. The specific electrophysiologic properties of all 257 nodes can be found after downloading the model from www.ecgsim.org (free of charge). With default parameter settings, ECGSIM generates an ECG that closely resembles the ECG of a healthy subject.

For the current study, the activation sequences associated with pacing were based on previously published depolarization maps.[20–24] Left posterolateral node no. 79 was selected as the LV epicardial pacing site. The averaged QRS duration measured in the heart failure patients was adopted as the total time of ventricular depolarization. The moment of activation of each node was calculated by multiplying the total time of depolarization by the ratio of the distance of each node from the pacing site to the total distance the activation front needed to travel to activate the entire heart. The action potential durations of all nodes were left unaltered. The repolarization times of all nodes were calculated by addition of the action potential durations to the moments of activation.

RV pacing was simulated in a similar manner. The heart was activated from RV apical endocardial node no. 249. Biventricular pacing was simulated by simultaneous pacing from nodes no. 79 and 249, thus combining the ventricular depolarization and repolarization times of LV and RV pacing. Thereafter, ECGSIM constructed isochrone maps of depolarization and repolarization times of the heart. The simulated ECGs were analyzed with the LEADS program as described earlier.

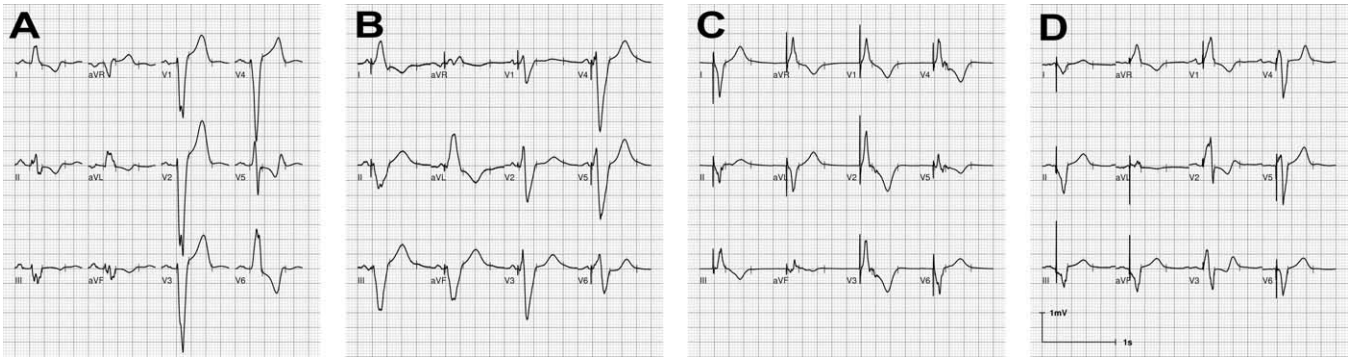

Figure 1 Sample ECGs (average beat) during sinus rhythm, right ventricular pacing, left ventricular pacing, and biventricular pacing. **A:** Subject 08 in sinus rhythm. **B:** Subject 26 during right ventricular pacing. **C:** Subject 19 during left ventricular pacing. **D:** Subject 07 during biventricular pacing.

For comparison with normal ventricular activation with an intact conduction system, we used the default settings of depolarization and repolarization times of ECGSIM, which generates a normal ECG.

We calculated TDR for the different pacing modes and during normal activation. Each endocardial node was paired with an opposing epicardial node, and TDR was calculated as the difference in repolarization time between the endocardial and epicardial node.[25] Because there are more epicardial nodes than endocardial nodes, several endocardial nodes had two opposing epicardial nodes. In these cases, the difference was calculated between the repolarization time of the endocardial node and the mean repolarization time of the two opposing epicardial nodes. Similarly, each LV septal node was paired with one or two RV septal nodes. Subsequently, all paired repolarization time differences were averaged to calculate TDR. In addition, we measured local TDR directly under the LV epicardial pacing site during LV pacing and during normal ventricular activation. Similarly, local TDR in the septum directly under the RV endocardial pacing site was calculated.

Statistical analysis

Repeated measures ANOVA was performed before post hoc t-testing. Two-sided paired t-tests were used to compare data between different pacing modes. P values were Bonferroni corrected for multiple testing. $P < .05$ was considered significant.

Results

Patients

Four ECGs recorded during sinus rhythm, RV pacing, LV pacing, and biventricular pacing are shown in Figure 1. All ECGs were highly discordant: QRS- and T-wave polarities were opposite in almost all leads of every rhythm. Consequently, the spatial angles between the QRS and T axes (a gross qualifier of concordance / discordance) were close to 180° (Table 2A). The largest average spatial QRS-T angle was attained during RV pacing. Correlation coefficients of the spatial orientation of the QRS and T vectors were 0.96 for RV pacing, 0.79 for LV pacing, and 0.85 for biventricular pacing.

Table 2A lists average heart rate, QRS duration, and the values of ECG indices of dispersion of repolarization. QRS duration was longest during RV pacing and shortest during biventricular pacing. LV pacing had intermediate values (see Table 2B for P values). QTc and Tapex–end$_c$ intervals followed the same pattern, with decreasing values from RV to LV and biventricular pacing. The same applies to T-wave amplitude and area. The pattern present in the ECG indices during different rhythms is shown in Figure 2. T-wave complexity was large during biventricular pacing and small during RV pacing.

Simulations

Depolarization and repolarization maps are shown in Figure 3. The maps of the normal situation with intact conduction system are shown in panel A, in which depolarization and repolarization patterns differ significantly. During RV and LV pacing (panels B and C), depolarization spreads from the RV apex and the LV lateral wall, respectively. Here, repolarization roughly follows the depolarization pattern. During biventricular pacing (panel D), the heart is activated simultaneously from these two sites. Here the repolarization map also resembles the depolarization map.

The corresponding simulated ECGs are shown in Figure 4. During normal ventricular activation (panel A), the ECG is normal and highly concordant: the QRS complex and the T wave had similar polarity in most leads. In all pacing modes, the ECGs were highly discordant: the QRS complex and the T wave had opposite polarities in most leads. The spatial angle between the QRS and T axes was small during normal ventricular activation and close to 180° during pacing.

Table 3 lists the main characteristics of the simulated ECGs. The values of all ECG repolarization indices were smallest during normal ventricular activation. QRS duration was longest for RV pacing, smaller for LV pacing, smallest for biven-

Table 2A ECG characteristics of heart failure patients during different rhythms

ECG characteristic	Sinus rhythm	Right ventricular pacing	Left ventricular pacing	Biventricular pacing
Heart rate (bpm)	73 ± 11	72 ± 14	72 ± 12	73 ± 11
QRS duration (ms)	175 ± 31	191 ± 31	167 ± 36	146 ± 17
QTc (ms)	503 ± 47	512 ± 45	487 ± 31	477 ± 44
Tapex–end$_c$ (ms)	108 ± 27	117 ± 22	106 ± 21	102 ± 18
Tamplitude (μV)	362 ± 219	478 ± 174	335 ± 143	287 ± 125
Tarea (μV · s)	66 ± 31	94 ± 35	62 ± 26	56 ± 22
Tcomplexity	0.30 ± 0.13	0.25 ± 0.10	0.36 ± 0.19	0.42 ± 0.26
QRS-T angle (°)	162 ± 20	167 ± 9	149 ± 28	154 ± 21

Data are given as average ± SD.

tricular pacing. QTc was longest for RV pacing and smaller during LV and biventricular pacing. Tapex–end$_c$ interval was longest for RV pacing and smaller for LV and biventricular pacing. T-wave amplitude and area decreased from RV to LV to biventricular pacing. T-wave complexity was largest during biventricular pacing. QRS-T angle was largest during RV pacing and decreased from LV to biventricular pacing but remained relatively large.

In ECGSIM, TDR in the whole heart and in the LV free wall was larger during pacing than during normal ventricular activation with intact conduction system, but differences between pacing modes were small. TDR in the whole heart was largest for RV pacing (29 ms) and slightly smaller for LV pacing (26 ms) and biventricular pacing (27 ms). TDR was 18 ms during normal conduction. TDR in the LV free wall showed the same pattern with slightly higher values: 36 ms for RV pacing, 31 ms for LV pacing, and 32 ms for biventricular pacing, with a TDR of 19 ms for a normally conducted beat.

Local TDR directly under the LV pacing site increased from 18 ms during normal ventricular activation to 39 ms during LV epicardial pacing, as a result of the reversal of the naturally existing endocardial to epicardial activation order. In the septum directly under the RV pacing site, local TDR increased from 20 to 75 ms during RV endocardial pacing.

Discussion

Our simulations indicate that TDR during LV and biventricular pacing was not larger than TDR during conventional RV endocardial pacing, neither in the whole heart nor directly under the pacing sites. In patients treated with CRT, ECG indices of dispersion of repolarization were measured during different pacing modes. The observed magnitudes of these ECG indices can be explained by interpretation of our simulations.

Table 2B *P* values for all ECG differences between different pacing modes

ECG characteristics	RV vs LV pacing	LV vs BIV pacing	BIV vs RV pacing
Heart rate (bpm)	1	1	1
QRS duration (ms)	.002	.004	<.0001
QTc (ms)	.005	1	.003
Tapex–end$_c$ (ms)	.0009	1	.005
Tamplitude (μV)	.0006	.6	<.0001
Tarea (μV · s)	.0006	1	<.0001
Tcomplexity	.048	1	.004
QRS-T angle (°)	.02	1	.008

BIV = biventricular; LV = left ventricular; RV = right ventricular.

Principles of repolarization during pacing

In the virtual situation where all myocardial cells depolarize at the same instant, only intrinsic differences in action potential duration would determine the repolarization sequence. During normal ventricular activation, there is a mix of conduction system-mediated rapid depolarization and slower cell-to-cell conduction. In such cases, the repolarization order is partly determined by the order in which the cells depolarize and partly by intrinsic action potential duration differences. In the paced heart, slow cell-to-cell conduction prevails,[20–24] and the repolarization order starts to closely resemble the depolarization order, a condition associated with secondary T-wave changes.[26]

In our patients, as well as in the paced simulations, the QRS complex and the T wave had opposite polarities, and

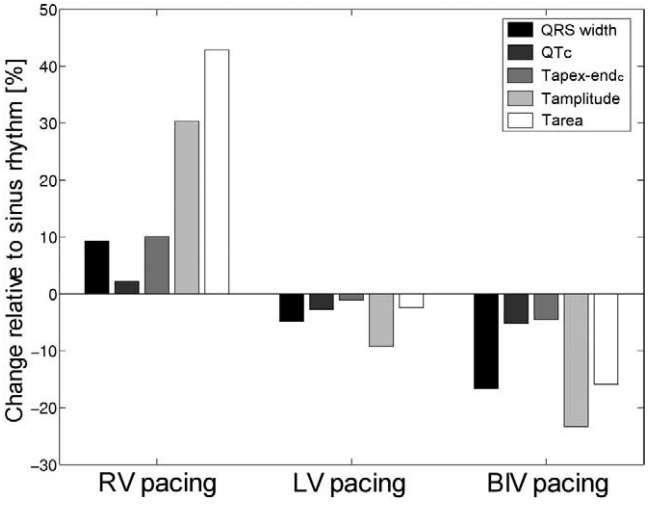

Figure 2 Values of ECG indices during right ventricular (RV), left ventricular (LV), and biventricular (BIV) pacing relative to sinus rhythm. Values of ECG indices decreased in magnitude from RV to LV to BIV pacing.

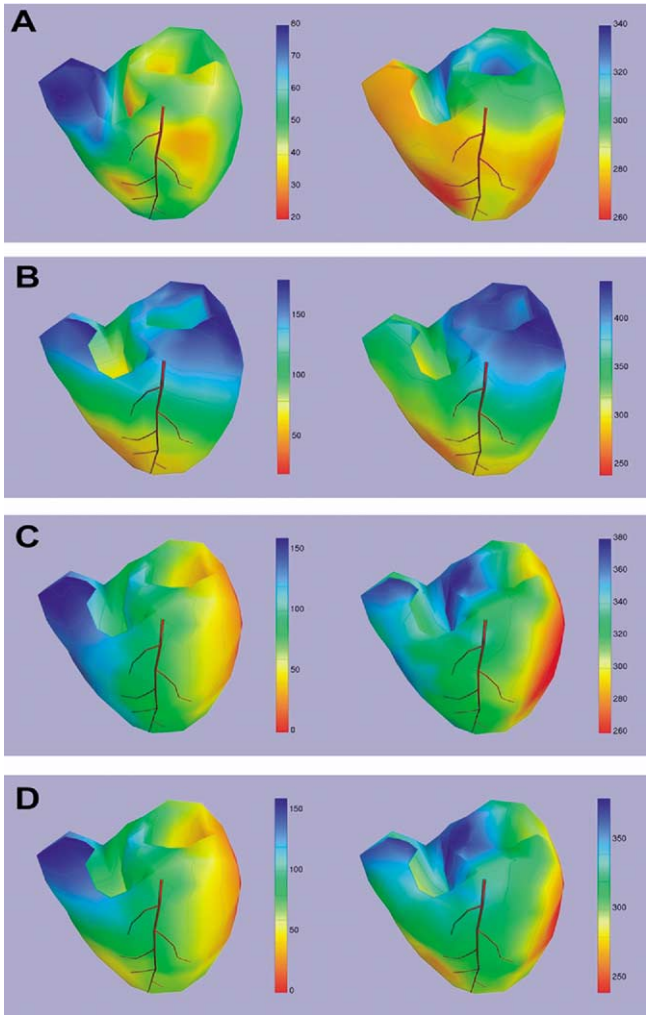

Figure 3 Simulated depolarization/repolarization maps. Hearts are depicted from the anterosuperior view with the left anterior descending artery as the landmark. *Red* indicates the earliest depolarization/repolarization, and *blue* indicates the latest depolarization/repolarization. **A:** Normal ventricular activation, intact conduction system. **B:** Right ventricular endocardial pacing. Apparently, the repolarization pattern is now very similar to the depolarization pattern. **C:** Left ventricular epicardial pacing. The repolarization pattern closely resembles the depolarization pattern. **D:** Biventricular pacing.

the spatial angle between QRS and T axes approximated 180°. Such discordant ECGs emerge when the repolarization sequence roughly equals the depolarization sequence. The opposite polarity is caused by the opposite direction of repolarizing and depolarizing currents. This view is supported by the simulated ECGs (Figure 4) that strikingly resemble the ECGs recorded in patients (Figure 1). These ECGs could be generated only by changing the ventricular depolarization sequence while leaving the action potential durations unaffected.

The discordance between QRS complex and T wave during pacing is in contrast to the concordance found in the simulated ECGs during normal activation (Figure 4A). During normal activation, the epicardium depolarizes last but repolarizes first because of the relatively short epicardial action potential durations. In combination with the opposite direction of depolarizing and repolarizing currents, concordant QRS complex and T wave emerge.

Transmural dispersion of repolarization

In accordance with the findings of Medina-Ravell et al,[6] ECGSIM showed an increased transmural repolarization gradient directly under the LV pacing site during LV pacing. However, TDR in the septum directly under the RV apical pacing site during RV pacing also was increased. This finding is not entirely unexpected because, like the epicardial LV lead, the endocardial RV lead is located outside the LV.

Average TDR in the whole-heart model was approximately the same during all pacing modes and slightly increased compared with normal activation (29, 26, 27, and 18 ms during RV pacing, LV pacing, biventricular pacing and normal activation, respectively). This can be explained by the repolarization maps (Figure 3). During pacing (panels B–D), the depolarization sequence is followed by a similarly shaped repolarization pattern that spreads from the pacing site through the ventricles. With increasing distance from the pacing site, the epicardial to endocardial activation order, which accentuates local TDR, is lost. For example, observe the depolarization wavefront at the basal surface of the LV during LV pacing (panel C). The major part of the LV base is depolarized by a wavefront that progresses in a direction approximately parallel to the ventricular walls. Such a depolarization order does not introduce a large TDR because it does not advance the depolarization time of the epicardium compared with the endocardium. Both LV epicardial and RV endocardial pacing create such transventricular depolarization and repolarization patterns. Other than their opposite direction, these patterns are not essentially different from another. Although biventricular pacing is performed from two pacing sites, similar transventricular repolarization patterns are induced in the greater part of the ventricles (panel D). Hence, TDR is similar during all pacing modes. However, the efficiency of an intact conduction system with well-synchronized endocardial to epicardial activation throughout the heart is not attained by any pacing mode. Therefore, TDR is moderately larger during all pacing modes than during sinus rhythm.

Tapex–end interval

The Tapex–end interval is a measure of TDR in the wedge preparation of the LV free wall.[8] The apex of the T wave emerges when the transmural voltage gradients are maximal, that is, when epicardial action potentials have their steepest decline in amplitude. This was elegantly shown by Antzelevitch et al.[8] In a recent publication it was reported that the Tapex–end interval was increased in ECGs of heart failure patients during LV pacing. Based on the assumption

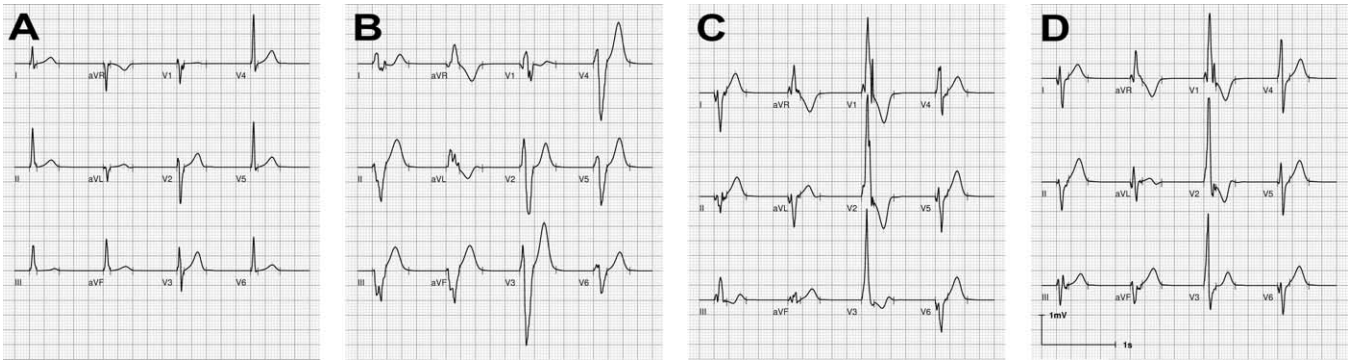

Figure 4 ECGs generated by ECGSIM. **A:** Normal ventricular activation, intact conduction system. **B:** Right ventricular pacing. **C:** Left ventricular pacing. **D:** Biventricular pacing.

that the laboratory situation (wedge) and the clinical situation (whole heart) are analogous, LV pacing was concluded to increase TDR.[6]

Our simulations suggest that other factors determine the Tapex–end interval during pacing of a whole heart. The occurrence of the apex of the T vector can be understood from the repolarization maps in Figure 3. During RV pacing (panel B), the repolarization wavefront increases in size when progressing from apex to base. The wavefront extends to its maximal area when it reaches the RV base of the heart (t = 342 ms, green isochrone). At that moment, the apex of the T vector emerges. During LV pacing (panel C), the repolarization wavefront has the largest area at 320 ms (green isochrone). However, at that moment, repolarization has already progressed to the RV before the repolarization of the septum is completed, which implies a certain amount of cancellation. This effect causes a relatively early occurrence (t = 300 ms, yellow isochrone) of the maximal T vector during LV pacing.

The end of the T vector occurs when the repolarization wavefronts have traveled to the most distant areas of the heart. In RV pacing, the final repolarization occurs at the LV base. In the case of LV pacing, the epicardium of the RV free wall is the last area to repolarize. Final repolarization in both RV and LV pacing occurs in parts of the heart that are relatively distant from the area that generates the maximal repolarization vector. Therefore, neither the Tapex–end interval during RV pacing nor the Tapex–end interval during LV pacing expresses TDR. Thus, during pacing, the Tapex–end interval contains information on the global transventricular repolarization process, whereas local repolarization differences in adjacent regions, like TDR, are considered more arrhythmogenic.[27,28]

T-wave amplitude

Studies in biologic and mathematical models relate increased T-wave amplitude to increased dispersion of repolarization. Increased TDR induced by hyperkalemia[29] or experimental long QT1 conditions[30] increases T-wave amplitude. In ECGSIM experiments, the T-wave amplitude increased with enhanced dispersion of repolarization.[13,25]

Hence, increased dispersion of repolarization during regular, conduction-system mediated ventricular activation may cause high-amplitude T waves. However, in the present study, high-amplitude T waves occurred during abnormal, cell-to-cell activation as a result of pacing. During pacing, TDR is relatively normal. The higher T-wave amplitude is caused by less cancellation because of the asymmetric depolarization and repolarization sequence.

Of the different pacing modes, biventricular pacing caused the lowest T-wave amplitude in our simulations and patients, as this pacing mode involves more cancellation because of the opposite directions of the two simultaneously started wavefronts (Figure 3D).

T-wave area

Several studies relate T-wave area to dispersion of repolarization. In rabbit hearts, dispersion of epicardial monophasic action potential duration was accompanied by increased T-wave area on a simultaneously recorded surface ECG.[14] In dogs, T-wave[31] and QRST[32] surface area were related to dispersion of repolarization and a lowered threshold for ventricular fibrillation.[33] We measured the smallest T-wave area during biventricular pacing compared with other pacing modes in patients and in our simulations. The low T-wave area during biventricular pacing resulted from cancellation because of the opposite directions of the two simultaneously started wavefronts and not because of increased TDR.

T-wave complexity

Increased T-wave complexity in patients with arrhythmogenic RV dysplasia is associated with arrhythmias.[34] Patients with long QT syndrome can be distinguished from healthy subjects by an increased T-wave complexity.[15] In US veterans with cardiovascular disease, repolarization complexity calculated with singular value decomposition conferred independent prognostic information.[35] Van Oosterom[36] showed mathematically that T-wave complexity was related to dispersion of

Table 3 Characteristics of simulated ECGs

	Normal conduction	Right ventricular pacing	Left ventricular pacing	Biventricular pacing
Heart rate (bpm)	60	60	60	60
QRS duration (ms)	100	184	172	166
QTc (ms)	376	450	401	400
Tapex–end$_c$ (ms)	79	104	93	94
Tamplitude (μV)	294	820	679	606
Tarea ($\mu V \cdot s$)	36	115	91	80
Tcomplexity	0.13	0.23	0.19	0.36
QRS-T angle (°)	69	168	151	147

repolarization induced by accentuated action potential duration differences. In our study, the largest T-wave complexity was found during biventricular pacing in heart failure patients and in the simulations. This is caused by the more complex repolarization pattern as a result of two colliding activation wavefronts instead of one. However, as stated earlier, the transventricular repolarization patterns and TDR are not essentially different from single-sided LV or RV pacing. Therefore, increased T-wave complexity in biventricular paced patients cannot be interpreted as an indication of increased arrhythmogeneity.

Study limitations

Like every modeling study, the simulations with ECGSIM are a simplification of reality. The model used is not specifically designed as a heart failure model. On the heart failure model and lacks complex alterations in anatomy and electrophysiology present in varying degrees in heart failure patients recent mapping studies in heart failure patients during pacing and sinus rhythm show individually variable areas of slow conduction[37] and lines of functional block[38] resulting in complex depolarization patterns. However, also in these studies, the largest areas were chiefly activated by slowly progressing wavefronts, suggesting myocardial cell-to-cell conduction, as we used in our simulations. We were able to simulate realistic ECGs in a model that was not primarily designed for the current study. ECGSIM has been extensively evaluated and is sufficiently realistic to show the principles of repolarization and its effects on the ECG.[13,39]

Conclusion

In patients treated with CRT, ECG repolarization indices are related to pacing-induced activation sequences rather than transmural dispersion of the repolarization. TDR during biventricular and LV pacing is not larger than TDR during conventional RV endocardial pacing.

Acknowledgments

This study was supported by the Netherlands Heart Foundation (grant 2001.177). Mortara Rangoni Europe, Italy, provided the ST Surveyor used for ECG recording.

References

1. Abraham WT, Fisher WG, Smith AL, DeLurgio DB, Leon AR, Loh E, Kocovic DZ, Packer M, Clavell AL, Hayes DL, Ellestad M, Trupp RJ, Underwood J, Pickering F, Truex C, McAtee P, Messenger J. Cardiac resynchronization in chronic heart failure. N Engl J Med 2002;346:1845–1853.
2. John Sutton MG, Plappert T, Abraham WT, Smith AL, DeLurgio DB, Leon AR, Loh E, Kocovic DZ, Fisher WG, Ellestad M, Messenger J, Kruger K, Hilpisch KE, Hill MR. Effect of cardiac resynchronization therapy on left ventricular size and function in chronic heart failure. Circulation 2003;107:1985–1990.
3. Bradley DJ, Bradley EA, Baughman KL, Berger RD, Calkins H, Goodman SN, Kass DA, Powe NR. Cardiac resynchronization and death from progressive heart failure: a meta-analysis of randomized controlled trials. JAMA 2003;289:730–740.
4. Cleland JGF, Daubert J, Erdmann E, Freemantle N, Gras D, Kappenberger L, Tavazzi L. The effect of cardiac resynchronization on morbidity and mortality in heart failure. N Engl J Med 2005;352:1539–1549.
5. Fish JM, Di Diego JM, Nesterenko V, Antzelevitch C. Epicardial activation of left ventricular wall prolongs QT interval and transmural dispersion of repolarization: implications for biventricular pacing. Circulation 2004;109:2136–2142.
6. Medina-Ravell VA, Lankipalli RS, Yan GX, Antzelevitch C, Medina-Malpica NA, Medina-Malpica OA, Droogan C, Kowey PR. Effect of epicardial or biventricular pacing to prolong QT interval and increase transmural dispersion of repolarization: does resynchronization therapy pose a risk for patients predisposed to long QT or torsade de pointes? Circulation 2003;107:740–746.
7. Yan GX, Lankipalli RS, Burke JF, Musco S, Kowey PR. Ventricular repolarization components on the electrocardiogram: cellular basis and clinical significance. J Am Coll Cardiol 2003;42:401–409.
8. Yan GX, Antzelevitch C. Cellular basis for the normal T wave and the electrocardiographic manifestations of the long-QT syndrome. Circulation 1998;98:1928–1936.
9. Cowan JC, Hilton CJ, Griffiths CJ, Tansuphaswadikul S, Bourke JP, Murray A, Campbell RW. Sequence of epicardial repolarisation and configuration of the T wave. Br Heart J 1988;60:424–433.
10. Franz MR, Bargheer K, Rafflenbeul W, Haverich A, Lichtlen PR. Monophasic action potential mapping in human subjects with normal electrocardiograms: direct evidence for the genesis of the T wave. Circulation 1987;75:379–386.

11. Van Oosterom A, Oostendorp TF. ECGSIM: an interactive tool for studying the genesis of QRST waveforms. Heart 2004;90:165–168.
12. Moss AJ. Measurement of the QT interval and the risk associated with QTc interval prolongation: a review. Am J Cardiol 1993;72: 23–25.
13. Van Oosterom A. Genesis of the T wave as based on an equivalent surface source model. J Electrocardiol 2001;34:S217–S127.
14. Zabel M, Portnoy S, Franz MR. Electrocardiographic indexes of dispersion of ventricular repolarization: an isolated heart validation study. J Am Coll Cardiol 1995;25:746–752.
15. Priori SG, Mortara DW, Napolitano C, Diehl L, Paganini V, Cantu F, Cantu G, Schwartz PJ. Evaluation of the spatial aspects of T-wave complexity in the long-QT syndrome. Circulation 1997;96: 3006–3012.
16. Bazett HC. An analysis of the time relation of electrocardiograms. Heart 1920;7:353–367.
17. Lay DC. Linear algebra and its applications. Second edition. Reading, MA: Addison-Wesley, 2003:441-486.
18. Dower GE, Machado HB, Osborne JA. On deriving the electrocardiogram from vectoradiographic leads. Clin Cardiol 1980;3:87–95.
19. Edenbrandt L, Pahlm O. Vectorcardiogram synthesized from a 12-lead ECG: superiority of the inverse Dower matrix. J Electrocardiol 1988; 21:361–367.
20. Faris OP, Evans FJ, Dick AJ, Raman VK, Ennis DB, Kass DA, McVeigh ER. Endocardial versus epicardial electrical synchrony during LV free-wall pacing. Am J Physiol Heart Circ Physiol 2003;285: H1864–H1870.
21. Reddy VY, Neuzil P, Taborsky M, Kralovec S, Sediva L, Ruskin JN. Images in cardiovascular medicine. Electroanatomic mapping of cardiac resynchronization therapy. Circulation 2003;107:2761–2763.
22. Scher AM, Young AC. Spread of excitation during premature ventricular systoles. Circ Res 1955;3:535–542.
23. Spach MS, Barr RC. Analysis of ventricular activation and repolarization from intramural and epicardial potential distributions for ectopic beats in the intact dog. Circ Res 1975;37:830–843.
24. Vassallo JA, Cassidy DM, Miller JM, Buxton AE, Marchlinski FE, Josephson ME. Left ventricular endocardial activation during right ventricular pacing: effect of underlying heart disease. J Am Coll Cardiol 1986;7:1228–1233.
25. Hooft van Huysduynen B, Swenne CA, Draisma HH, Antoni ML, Van de Vooren H, Van der Wall EE, Schalij MJ. Validation of ECG indices of ventricular repolarization heterogeneity: a computer simulation study. J Cardiovasc Electrophysiol, 2005;16:1097–1103.
26. Wilson FN, MacLeod AG, Barker PS. The T deflection of the electrocardiogram. Trans Assoc Am Physicians 1931;46:29–38.
27. Akar FG, Yan GX, Antzelevitch C, Rosenbaum DS. Unique topographical distribution of M cells underlies reentrant mechanism of torsade de pointes in the long-QT syndrome. Circulation 2002;105: 1247–1253.
28. El Sherif N, Caref EB, Chinushi M, Restivo M. Mechanism of arrhythmogenicity of the short-long cardiac sequence that precedes ventricular tachyarrhythmias in the long QT syndrome. J Am Coll Cardiol 1999;33:1415–1423.
29. Litovsky SH, Antzelevitch C. Transient outward current prominent in canine ventricular epicardium but not endocardium. Circ Res 1988; 62:116–126.
30. Shimizu W, Antzelevitch C. Cellular basis for the ECG features of the LQT1 form of the long-QT syndrome: effects of beta-adrenergic agonists and antagonists and sodium channel blockers on transmural dispersion of repolarization and torsade de pointes. Circulation 1998; 98:2314–2322.
31. Van Opstal JM, Verduyn SC, Winckels SK, Leerssen HM, Leunissen JD, Wellens HJ, Vos MA. The JT-area indicates dispersion of repolarization in dogs with atrioventricular block. J Interv Card Electrophysiol 2002;6:113–120.
32. Abildskov JA, Green LS, Evans AK, Lux RL. The QRST deflection area of electrograms during global alterations of ventricular repolarization. J Electrocardiol 1982;15:103–107.
33. Kubota I, Lux RL, Burgess MJ, Abildskov JA. Relation of cardiac surface QRST distributions to ventricular fibrillation threshold in dogs. Circulation 1988;78:171–177.
34. De Ambroggi L, Aime E, Ceriotti C, Rovida M, Negroni S. Mapping of ventricular repolarization potentials in patients with arrhythmogenic right ventricular dysplasia: principal component analysis of the ST-T waves. Circulation 1997;96:4314–4318.
35. Zabel M, Malik M, Hnatkova K, Papademetriou V, Pittaras A, Fletcher RD, Franz MR. Analysis of T-wave morphology from the 12-lead electrocardiogram for prediction of long-term prognosis in male US veterans. Circulation 2002;105:1066–1070.
36. Van Oosterom A. Singular value decomposition of the T wave: its link with a biophysical model of repolarization. Int J Bioelectromagnetism 2002;4:59–60.
37. Lambiase PD, Rinaldi A, Hauck J, Mobb M, Elliott D, Mohammad S, Gill JS, Bucknall CA. Non-contact left ventricular endocardial mapping in cardiac resynchronisation therapy. Heart 2004;90:44–51.
38. Auricchio A, Fantoni C, Regoli F, Carbucicchio C, Goette A, Geller C, Kloss M, Klein H. Characterization of left ventricular activation in patients with heart failure and left bundle-branch block. Circulation 2004;109:1133–1139.
39. van Oosterom A. The dominant T wave and its significance. J Cardiovasc Electrophysiol 2003;14:S180–S187.